NOVEL SILICA/POLYELECTROLYTE MULTILAYER CORE-SHELL COMPOSITE MICROPARTICLES WITH SELECTIVITY FOR ANIONIC DYES

CLAUDIU-AUGUSTIN GHIORGHITA, FLORIN BUCATARIU and
ECATERINA STELA DRAGAN

"Petru Poni" Institute of Macromolecular Chemistry, 41A, Grigore Ghica Voda Alley,
700487 Iasi, Romania
✉ *Corresponding author: Ecaterina Stela Dragan, sdragan@icmpp.ro*

Dedicated to the 70th anniversary of
Acad. Bogdan C. Simionescu

In this paper, novel core-shell composites were fabricated by the deposition of polyelectrolyte multilayer films based on chitosan and poly(*N*,*N*-dimethylamino)ethyl methacrylate partially quaternized with benzyl chloride, as polycations, and carboxymethyl cellulose as polyanion onto silica microparticles. After construction, the films were cross-linked with a dihalogenated aromatic derivative. The role of polyelectrolyte deposition solutions in charge balance and morphology of the composites was investigated by potentiometric titrations and scanning electron microscopy, respectively. The new composites were tested as sorbents for four organic dyes (methylene blue, methyl orange, bromocresol green and Congo red), showing better sorption capacity for the anionic compounds. An insight into the sorption mechanisms of anionic dyes was obtained by fitting the equilibrium sorption isotherms with the Langmuir and Freundlich models, and the sorption kinetics with the pseudo-first order and pseudo-second order models. The optimum pH conditions for desorption of the dyes were also assessed. These results provide important information on the design of multilayer films containing diverse building-blocks on colloidal cores capable to selectively load ionic species.

Keywords: polyelectrolyte multilayer films, chitosan, carboxymethyl cellulose, dye sorption

INTRODUCTION

One of the directions considered for the reduction of human impact on environmental degradation is the decontamination of domestic and industrial wastewaters by the removal of all sorts of pollutants (heavy metal ions, dyes, drugs, colloidal particles and biological matter).[1] Current research in this field is directed towards: (i) the development of membrane separation techniques[2-4] and (ii) the design of sorbents capable of retaining large amounts of contaminants.[5,6] Membrane separation techniques are basically filtration processes, in which solutes from different mixtures are separated based on their molecular weight cut-off. However, membranes suffer from several drawbacks which impede their large scale application, such as surface fouling, decrease of stability under prolonged use and reduced permittivity for enhancing the selectivity for certain solutes.[7,8] On the other hand, new sorbents have gained great attention because of: (i) wide variety of materials used in the fabrication process, (ii) reusability in multiple sorption/desorption cycles, and (iii) environment friendly post-disposal.[9,10] According to their nature, sorbents can be inorganic, organic, or composites containing both organic and inorganic constituents. Also, they can be produced in various shapes, such as microparticles, gels, beads, or core-shell systems, depending on the intended application. Considering these aspects, the range of sorbents is very wide and includes materials such as activated carbon, metal oxides, ion exchange resins, or composites obtained by coating inorganic particles with polymeric films.[11-14]

Among the methods to coat solid surfaces with polymeric films, the layer-by-layer (LbL) assembly of oppositely charged polyelectrolytes is

a versatile and convenient strategy to obtain organic films with control at nanometric scale over the film architecture.[15-16] The LbL technique offers numerous possibilities to select the assembly building-blocks, to choose the underlying substrate and to tune the deposition conditions (pH, ionic strength, concentration).[17-22] Using this strategy, an enormous library of polyelectrolyte multilayer films has been designed, with potential applications in fields such as biomedicine, energy, catalysis and separation science.[23-29]

In our group, numerous efforts have been devoted to the design of core-shell (inorganic core and organic shell) composite microparticles based on the deposition of various polyelectrolyte multilayer systems onto silica microparticles.[14,30-32] The resulting composites were investigated as matrices for sorption and release of organic compounds, such as dyes, drugs and proteins/enzymes. Parameters such as the number of deposited polyelectrolyte layers, the assembly conditions (polyelectrolyte concentration, pH and ionic strength), rinsing conditions and cross-linking nature have been found to play significant roles in controlling the sorption/release properties of compounds in/from the designed multilayer matrices.

Herein we investigate the construction of a new core-shell composite system by the deposition of a more particular multilayer architecture onto silica microparticles, and assess its interaction capacity with several organic dyes. For the multilayer film deposition, sodium carboxymethyl cellulose (CMC) was used as polyanion, while chitosan (CHI) and poly(*N*,*N*-dimethylamino)ethyl methacrylate partially quaternized with benzyl chloride (Q50PDMAEMA)[33] were used as polycations. The multilayer architecture consisted of five polyelectrolyte layers disposed as follows: CHI was the first and the last layer deposited, CMC was deposited as the second and the fourth layer, while the third layer (the central layer of the film) consisted of Q50PDMAEMA. We adopted this strategy to generate a symmetric composite multilayer film, which has never been investigated before. After construction, the LbL film was cross-linked with a dihalogenated aromatic compound. The influence of polyelectrolyte solution concentration on the LbL film formation was assessed by potentiometric titration, while the morphology of the resulting composites was investigated by scanning electron

microscopy (SEM). The novel composites were used as sorbents for four model organic dyes [methylene blue (MB), methyl orange (MO), bromocresol green (BCG) and Congo red (CR)]. The influence of dye nature, dye concentration and contact time on the sorption capacity of composites was investigated by UV-Vis measurements. Moreover, the optimum pH conditions for dye desorption were assessed.

EXPERIMENTAL
Materials

CHI (average M_w = 207 kDa; deacetylation degree = 85%) and CMC (average M_w = 90 kDa; 0.7 carboxymethyl groups per anhydroglucose unit) were purchased from Sigma-Aldrich and were used without additional purification. Q50PDMAEMA (quaternization degree = 50%, average M_w= 60 kDa, and polydispersity index = 2) was synthesized, purified and characterized in our laboratory according to the procedure previously presented.[33] The cross-linker, α,α'-dichloro-p-xylene (DCX), was purchased from Fluka. The chemical structures of the polyelectrolytes and the cross-linker are presented in Figure 1.

Silica microparticles (Daisogel type; SP1000) with particle diameters of 40-60 μm and average pore diameters of 100 nm, purchased from Daiso Co. (Japan), were used as colloidal substrates for the deposition of the multilayer films. All the dyes (MB, MO, BCG, and CR) were purchased from Sigma and used as received. Millipore water, with a conductivity of 0.055 μS m^{-1}, was used in all the experiments.

Construction of core-shell silica/polyelectrolyte multilayer composites

The polyelectrolyte multilayer films consisting of CHI, CMC and Q50PDMAEMA were deposited onto silica microparticles from salt-free aqueous solutions. Polymer solutions were prepared at concentrations of 5×10^{-3} M and 10^{-2} M with respect to monomer repeat unit, and allowed to stabilize for 24 h before use. The silica microparticles were activated by a treatment with 1% NaHCO$_3$ aqueous solution before use. The silica microparticles were suspended in CHI solution and gently shaken for 60 min to allow the deposition of the first polyelectrolyte layer. Following separation by decantation, the silica/CHI composite microparticles were rinsed three times with water to remove the weakly attached polymer chains. Next, the composites were suspended in CMC solution and gently shaken for 60 min to facilitate the deposition of the second polyelectrolyte layer. After CMC deposition, the silica/CHI/CMC composites were separated by decantation and rinsed with water three times. The above procedure (deposition, separation, rinsing) was followed for subsequent assembly of other three polyelectrolyte layers in the order Q50PDMAEMA, CMC, CHI on top of the silica/CHI/CMC composites.

In the end, a five layer polyelectrolyte film, with the sequence CHI/CMC/Q50PDMAEMA/CMC/CHI, was deposited onto the silica microparticles (Fig. 2).
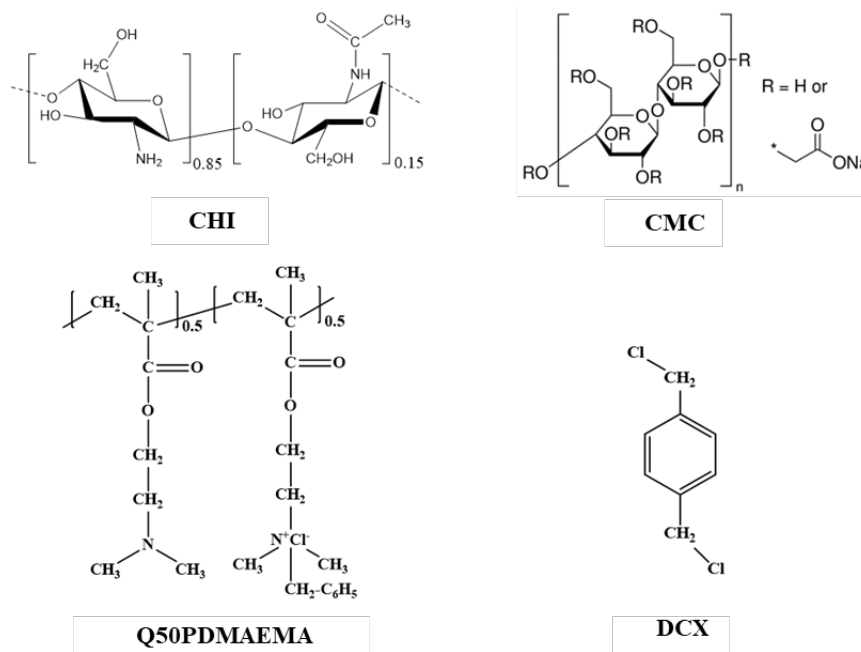

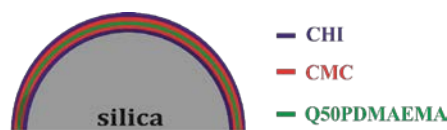Figure 1: Chemical structures of CHI, CMC, Q50PDMAEMA and DCX

Figure 2: Representation of the CHI/CMC/Q50PDMAEMA/CMC/CHI multilayer film deposited onto silica microparticles

Following the above strategy, two types of core-shell silica/polyelectrolyte multilayer composites were constructed, differing by the concentration of the polyelectrolyte solutions used in the assembly process (5×10^{-3} M and 10^{-2} M). The obtained composites were denoted with C1 and C2, respectively.

Cross-linking of polyelectrolyte multilayers

Cross-linking of the polyelectrolyte films was performed with DCX, according to a procedure presented elsewhere, with slight modifications.[34] Prior to cross-linking, a stock solution of DCX in acetone was prepared at a concentration of 10%. A certain amount of composite microparticles was suspended in fresh acetone up to saturation (minimum volume that completely covers the microparticles). Then, a corresponding volume of stock DCX solution was added dropwise under shaking, so that a cross-linker ratio of 2% (weight DCX/weight of composite microparticles × 100) was obtained. The reaction was conducted at room temperature for 24 h. After the completion of the reaction, the composite

microparticles were washed repeatedly with acetone and water, then dried in an oven at 40 °C under vacuum. The obtained cross-linked composites were denoted as C1R and C2R, corresponding to the samples prepared at polyelectrolyte concentrations of 5×10^{-3} M and 10^{-2} M, respectively.

Characterization methods

Potentiometric titrations were performed using a Particle Charge Detector (PCD-03) (Mütek GmbH, Germany) device in order to monitor the charge balance of the silica/polyelectrolyte multilayer composites after each deposition step. The pH was adjusted from the acidic range to the basic one using 0.1 M HCl and 0.1 M NaOH solutions. Potentiometric titrations give the point of zero charge (*pzc*) of the composite microparticles, which represents the pH where the measured potential is 0 mV.

Scanning electron microscopy (SEM) was used to investigate the morphology of the composite microparticles. An environmental scanning electron microscope (ESEM) type Quanta 200, operating at 20

kV, with secondary electrons in low vacuum mode, was employed.

UV-Vis measurements of different dye solutions were performed using a SPECORD 200 Analytic Jena UV-Vis spectrophotometer based on the calibration curve method.

Dye sorption/release experiments

Sorption/release experiments of different dyes onto/from the silica/polyelectrolyte multilayer composite microparticles were performed by a batch procedure. For sorption experiments, 25 mg composite microparticles were suspended in 10 mL dye solutions. The adsorbed amount of dyes (q_e) was quantified according to Eq. 1:

$$q_e = \frac{(C_0 - C_e) \cdot V}{m}$$

(1)

where C_0 = initial concentration of dye solution (mg/L); C_e = equilibrium concentration of dye in solution (mg/L); V = volume of dye solution (mL); m = amount of core-shell composite microparticles (mg).

Desorption experiments were performed at various pH conditions using NaOH solutions of different concentrations. Dye loaded composite microparticles (25 mg) were suspended in 10 mL release solutions for 1 h. Then, the supernatant was collected and the amount of released dyes was quantified by UV-Vis spectrophotometry.

RESULTS AND DISCUSSION
Construction of core-shell silica/polyelectrolyte multilayer composites

Nowadays, polymeric matrices are receiving more and more attention as sorbents for various environmental contaminants because they possess numerous functional groups that can interact with other molecules. Because inorganic materials, characterized by high mechanical stability, generally have a low interaction capacity with organic molecules, it is often common to functionalize them with polymers in order to enhance their sorption properties. In this context, the construction of a new core-shell composite system, comprising silica microparticles as inorganic core and a shell consisting of a symmetric composite multilayer film, with the sequence CHI/CMC/Q50PDMAEMA/CMC/CHI, having potential application as sorbents for organic dyes is investigated in this work. CHI contains a wealth of hydroxyl, amido and amino groups, CMC possesses numerous hydroxyl and carboxyl groups, while Q50PDMAEMA contains tertiary amine and quaternary ammonium salt moieties, which altogether are capable to interact with various pollutants. Herein, four organic dyes (MB, MO, BCG and CR) were chosen as model contaminants because their toxicity is well documented.[35,36]

It is known that each polyelectrolyte deposition step onto the underlying substrate leads to the modification of the surface charge balance, and, therefore, the surface charge of the silica microparticles was monitored by potentiometric titration measurements, after each deposition step, for both types of composites (C1 and C2) (Fig. 3).

In aqueous media, at pH $\geq$ 3, the surface of silica microparticles is negatively charged due to the presence of ionized silanol groups (Si-O⁻). These groups can establish electrostatic interactions with amino/ammonium groups of polycations. Therefore, the first layer deposited onto the silica microparticles consisted of CHI, a polycation that contains primary amino moieties. After CHI deposition, the *pzc* shifted to pH 6.7 and pH 8, for the C1 and C2 composites, respectively.
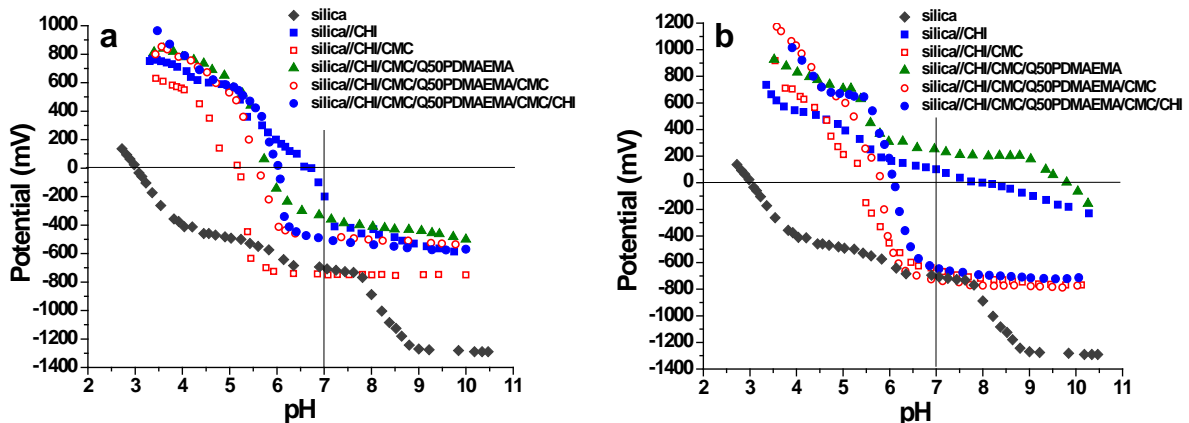

Figure 3: Potentiometric titrations of (a) C1 and (b) C2 composite microparticles after each polyelectrolyte deposition step onto the silica core
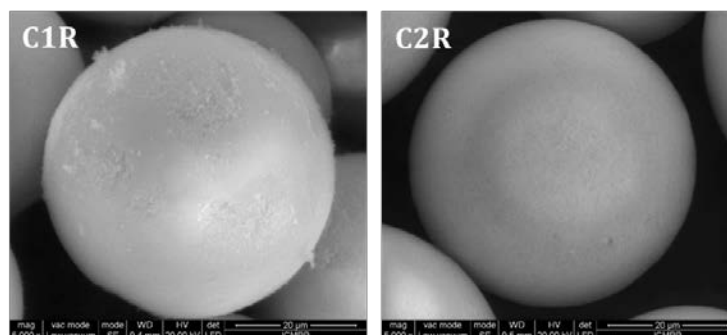
Figure 4: SEM images of C1R and C2R core-shell composite microparticles

The higher *pzc* of the C2 composite demonstrates that more amino groups are present on the surface of this composite, which can only be explained by the deposition of a higher amount of CHI chains.

When CMC was deposited onto the CHI covered silica microparticles, the *pzc* of the C1 and C2 composites decreased to pH 5.2 and pH 5.4, respectively. This shift in the *pzc* values demonstrates that CMC and CHI can be assembled in a layer-by-layer fashion based on electrostatic interactions between their functional groups. Further, the silica/CHI/CMC composites were suspended in Q50PDMAEMA solutions, a polycation that contains tertiary and quaternary amino moieties in equal proportion. The successful deposition of this polycation was provided by the *pzc* shift to pH 5.8 and pH 9.8, for the C1 and C2 composites, respectively. The significant higher *pzc* value of the C2 composite implies that a much higher number of amino groups are present on its surface, which can be attributed to the higher amount of polycation deposited when the polymer concentration is higher, as in the case of CHI deposition at higher concentration. The following deposited layer was again CMC, when the *pzc* decreased to pH = 5.6 and pH = 5.8 for the C1 and C2 composites, respectively. After the adsorption of another layer of CHI, only a slight increase of the *pzc* was observed for both composites (up to pH 6 and pH 6.1 for the C1 and C2 composites, respectively). This means that approximately the same amount of polycation was deposited in this step, irrespective of the polyelectrolyte concentration in the deposition solutions, and therefore we decided this to be the last layer adsorbed. This behaviour was also encountered for other polyelectrolyte multilayer systems, and can be attributed to the increasing distance from the underlying silica substrate, which leads to the equalization of the polyelectrolyte amount deposited in each assembly step.[37]

Cross-linking of multilayer architectures is a facile route to enhance the stability of films under extreme environmental conditions. Recently, our group demonstrated that multilayer films containing PDMAEMA can be cross-linked with DCX by the Menschutkin reaction, and the resulting films were more stable during repetitive treatments with NaOH solutions.[34] Herein, the same strategy was employed to cross-link the newly designed multilayer architecture. Unlike the previous study, in which PDMAEMA was the sole polycation, the multilayer system investigated in this study contains primary amino groups from CHI molecules, beside the tertiary amine from PDMAEMA, which can be involved in the cross-linking reaction. The morphology of the cross-linked composite core-shell microparticles was investigated by SEM (Fig. 4).

Both types of composite microparticles present spherical shape, due to the silica microparticle core. However, on a closer look, some differences can be seen on the microparticle surface, which can be attributed to the concentrations of the polyelectrolyte solutions used for the multilayer construction. The C1R composite system (Fig. 4, left image), which was constructed using the polyelectrolyte solutions of lower concentration (*i.e.* $5*10^{-3}$ M), presented numerous aggregates on the surface, suggesting that a non-uniform multilayer film was formed on the silica surface. Similar observations were made for other polysaccharide multilayer systems, which formed isolated islands when a low number of polyelectrolyte layers was deposited, while by the addition of more polyelectrolyte layers these
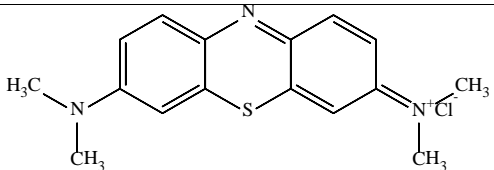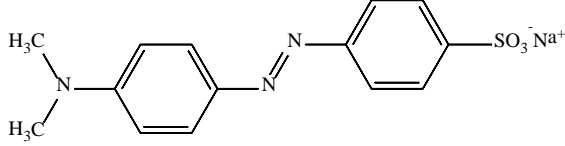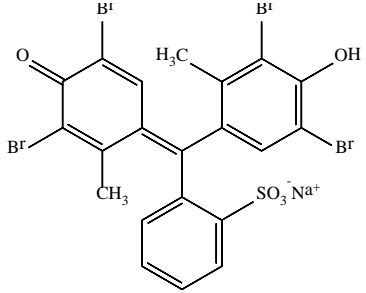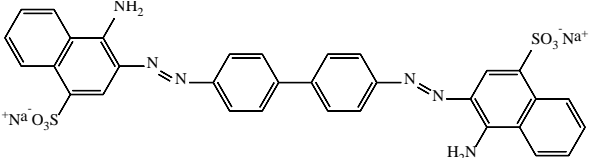
islands coalesced leading to uniform films.[38] To enhance the amount of polymeric material deposited onto the underlying substrate, the concentration of polyelectrolyte solutions used in the multilayer build-up was increased. As can be seen in Figure 4 (right image), the C2R composite system (in which the concentration of the polyelectrolyte solutions was 10^{-2} M) presented a uniform surface, which indicates that a homogeneous film was formed on the silica microparticles, thus confirming that this core-shell system contained a higher amount of organic material deposited.

Dye sorption/release experiments

To investigate the capacity of the designed core-shell silica/polyelectrolyte multilayer composite microparticles to sorb environmental contaminants, four organic dyes (MB as cationic dye and MO, BCG and CR as anionic species) were selected (Table 1).

First, a screening test was performed with all the dyes to assess which of them interacts better with the cross-linked core-shell composites (Table 2).

Table 1
Chemical structures, molar masses and maximum absorption wavelengths of MB, MO, BCG and CR

Dye	Chemical structure	Molar mass (g/mol)	λ_{max} (nm)
MB		319.85	665
MO		327.33	463
BCG		698.01	616[*]
CR		696.66	498

[*] in basic pH

Table 2
Sorption of organic dyes by C1R and C2R composite microparticles[*]

Sample	MB		MO		BCG		CR	
	C_o (mg/L)	q_e (mg/g)	C_o (mg/L)	q_e (mg/g)	C_o (mg/L)	q_e (mg/g)	C_o (mg/L)	q_e (mg/g)
C1R	27.58	0.50	51.85	1.05	46.95	5.23	47.57	5.21
C2R		0.11		3.93		11.06		9.22

[*] m = 25 mg; V = 10 mL, contact time = 2 h

It was found that MB was sorbed in a very low amount by the C1R and C2R composite microparticles, which indicates that the composites contain a low number of free anionic groups capable to electrostatically interact with the cationic groups of the dye. In comparison, the anionic dyes were sorbed in a much higher amount by the composite microparticles. The best sorption capacities were obtained when BCG and CR were tested, and therefore only these two dyes were used in the next sorption experiments. It is noteworthy that the C2R composite sorbed higher amounts of anionic dyes than the C1R system, which is attributed to the fact that more organic material was deposited onto the silica surface in this case.

The influence of dye concentration and contact time on the sorption of BCG and CR onto the C1R and C2R composite systems was assessed by sorption isotherms (Fig. 5) and kinetics experiments (Fig. 6).

As Figure 5 shows, the amounts of BCG and CR sorbed by the C1R and C2R composite systems increased gradually with the increase of dye concentration. All the isotherms fit a concave curve, which according to Limousin *et al.* can be classified as type "*L*" isotherms.[39] To obtain a mathematical prediction of the dye sorption processes onto both composites, the experimental sorption data were fitted using the non-linear regression forms of the Langmuir and Freundlich isotherm models.

The Langmuir isotherm is described by Equation 2:

$$q_e = \frac{q_m K_L C_e}{1 + K_L C_e}$$

(2)

where q_m is the maximum adsorption capacity when a surface is completely covered with a monolayer of sorbate molecules (mg/g) and K_L is the Langmuir constant (L/mg), which is related to the energy of adsorption.
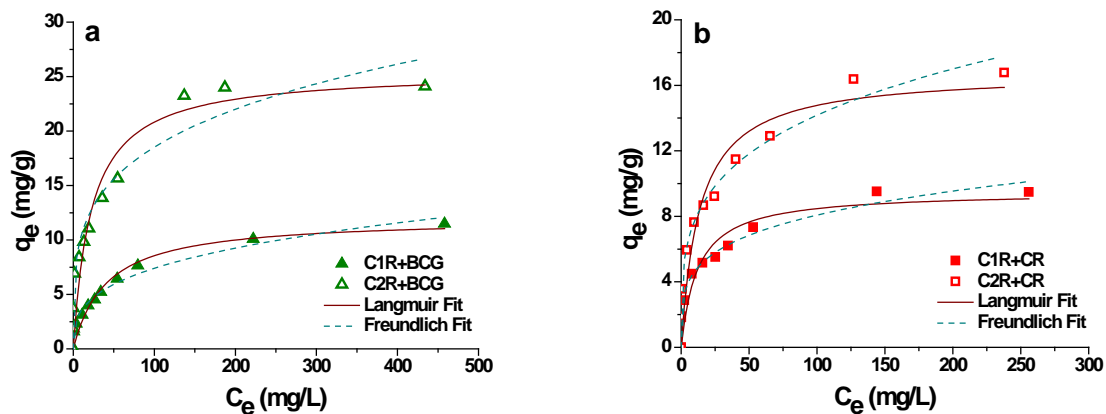

Figure 5: Equilibrium sorption isotherms for BCG and CR sorption onto C1R and C2R core-shell composite microparticles: m = 25 mg; V = 10 mL, t = 2 h
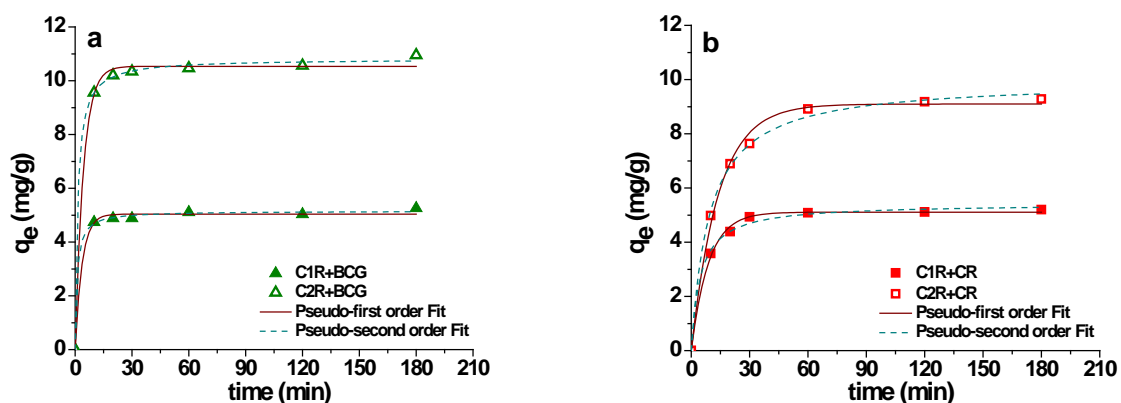

Figure 6: Pseudo-first order and pseudo-second order kinetic models applied for the equilibrium sorption of (a) BCG and (b) CR onto the C1R and C2R core-shell composite microparticles: m = 25 mg; V = 10 mL, q_o = 50 mg/L

Table 3

Parameters of Langmuir and Freundlich isotherms obtained by non-linear regression for BCG and CR sorption onto C1R and C2R core-shell composite microparticles

Parameter	C1R		C2R	
	BCG	CR	BCG	CR
q_e (mg/g)	11.48	9.49	24.11	16.78
Langmuir model				
q_m (mg/g)	12.02±0.72	9.49±0.79	25.48±2.01	16.78±1.34
K_L (L/mg)	0.03±0.01	0.66±0.28	0.05±0.01	0.07±0.02
R^2	0.959	0.901	0.911	0.914
χ^2	0.513	0.959	6.41	2.629
Freundlich model				
K_F (mg$^{1-1/n}$ L$^{1/n}$ g^{-1})	1.68±0.14	2.67±0.18	5.90±0.71	4.23±0.39
$1/n$	0.32±0.02	0.24±0.02	0.25±0.02	0.26±0.03
R^2	0.984	0.983	0.958	0.975
χ^2	0.204	0.165	3.016	0.766

The Freundlich isotherm is given by Equation 3:

$$q_e = K_F C_e^{1/n}$$ (3)

where K_F is the Freundlich constant, which gives an estimation of the amount of sorbate retained per gram of sorbent at the equilibrium concentration (mg$^{1-1/n}$ L$^{1/n}$ g^{-1}), and *n* is a measure of the nature and strength of the sorption process and the distribution of active sites related to the surface heterogeneity (the heterogeneity of the system increases with *n*).

The adsorption isotherm parameters obtained for the sorption of both dyes onto the C1R and C2R composite systems, as well as the correlation coefficients (R^2) and non-linear Chi-square test (χ^2) are given in Table 3.

The maximum sorption capacities for BCG and CR estimated by the Langmuir model (q_m) are 12.02±0.72 mg/g and 9.49±0.79 mg/g for the C1R composite, and 25.48±2.11 mg/g and 16.78±1.34 mg/g for C2R, respectively, which are in good agreement with the experimental values (Table 3). The Langmuir isotherm assumes monolayer sorption of solutes onto the adsorbent binding sites, which are considered energetically equivalent. However, the lower values of R^2 and the higher values of χ^2 indicate that the sorption of dyes onto the core-shell composites was only partially homogeneous and that the sorption sites were heterogeneously distributed in the polymeric LbL film.

The Freundlich isotherm model is used to describe the sorption process onto heterogeneous surfaces, under the assumption that the binding sites are not equivalent. As Table 3 shows, the values of R^2 and χ^2 obtained by modelling the

sorption of BCG and CR onto the core-shell composites with this isotherm model were the highest and the lowest, respectively, indicating that this model is the most appropriate to describe the sorption process, and that the surfaces of the composite are heterogeneous. The $1/n < 1$ values indicate that the binding energies increase with the surface density.

Concerning the influence of contact time on the sorption process, it was found that the time required to reach equilibrium sorption was approximately 20 min in the case of BCG for both composites, while in the case of CR it was approximately 30 min for the C1R composite, and approximately 120 min for the C2R system (Fig. 6).

The pseudo-first order (Eq. 4) and the pseudo-second order kinetic models (Eq. 5) were employed to evaluate the experimental sorption data of BCG and CR onto the C1R and C2R composite microparticles.

$$q_t = q_e (1 - e^{-k1t})$$ (4)

$$q_t = \frac{k_2 q_e^2 t}{1 + k_2 q_e t}$$ (5)

where q_e and q_t represent the amounts of dyes sorbed at equilibrium (mg/g) and at time *t*, respectively, k_1 is the rate constant of the pseudo-first order kinetic model (min^{-1}), and k_2 is the rate constant of the pseudo-second order kinetic model (g·mg^{-1}·min^{-1}). Table 4 lists the calculated parameter values corresponding to both kinetic models applied for the sorption of BCG and CR onto the C1R and C2R composites.

As Table 4 shows, the high values of R^2 and low values of χ^2 obtained by fitting both kinetic models on the experimental data of BCG and CR

sorption onto the core-shell composites indicate that both models are suitable to describe the sorption kinetics.

The release of BCG and CR from the composite microparticles as a function of pH was also studied (Fig. 7).

Table 4
Kinetic model parameters for BCG and CR sorption onto C1R and C2R core-shell composite microparticles

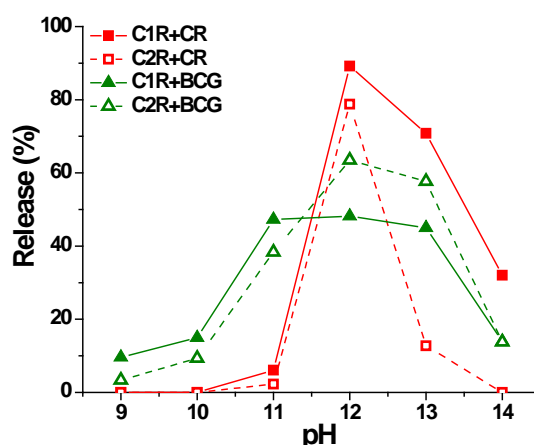| Parameter	C1R		C2R	
	BCG	CR	BCG	CR
$q_{e,exp}$ (mg/g)	5.23	5.21	11.06	9.22
Pseudo-first order model				
$q_{e,cal}$ (mg/g)	5.04±0.06	5.11±0.06	10.54±0.11	9.09±0.15
k_1 (min^{-1})	0.27±0.05	0.11±0.006	0.23±0.025	0.07±0.005
R^2	0.995	0.995	0.996	0.994
χ^2	0.019	0.019	0.053	0.063
Pseudo-second order model				
$q_{e,cal}$ (mg/g)	5.15±0.06	5.42±0.1	10.81±0.08	9.96±0.15
k_2 (g·mg^{-1}·min^{-1})	0.19±0.05	0.04±0.006	0.07±0.01	0.01
R^2	0.998	0.997	0.999	0.997
χ^2	0.008	0.012	0.016	0.033

Figure 7: Desorption of BCG and CR as a function of pH from C1R and C2R core-shell composite microparticles

At pH 9 and pH 10, CR was not desorbed at all from the composite microparticles, while the release of BCG was very poor. At these pH values, a small part of the amino groups of polycations are still ionized, therefore the release is prevented by the existence of electrostatic interactions between the sulfonate groups of the dyes and the ammonium groups in the polymeric matrix. The maximum CR desorption percentage was attained at pH 12, when the amino groups in the LbL films are completely uncharged. At this pH, the attractive forces between the anionic dye and the cross-linked films are suppressed, and the repulsive forces between the sulfonate groups of the dyes and the ionized carboxylic groups from the LbL matrix make the desorption faster. For BCG, a lower release percentage, but in a larger pH interval (pH 11-13), was obtained, which

could be due to the existence of hydrophobic interactions between the dye molecules and polysaccharide chains. Increasing the pH of the system leads to an increase in the amount of Na$^+$ ions, which decreases the electrostatic repulsion between the anionic groups of the dyes and the LbL films. In this way, Na$^+$ acts as a bridge between sulfonates and carboxylic groups, reducing the desorbed amount of the dyes at extreme basic pH.

CONCLUSION

Core-shell composites based on a symmetric composite multilayer film with the sequence CHI/CMC/Q50PDMAEMA/CMC/CHI, deposited onto silica microparticles, were prepared in this study. After construction, the multilayer films were stabilized by cross-linking with a

dihalogenated aromatic compound. The concentration of the polyelectrolyte solution used in the assembly of organic films showed a strong influence on charge balance, morphology and dye sorption capacities of the obtained composites. The composites obtained using the polyelectrolyte solution concentration of 10^{-2} M exhibited a smooth surface morphology, indicating the formation of a uniform, continuous multilayer film. The composites presented a very low sorption capacity for cationic dye (MB), but anionic dyes were sorbed in significantly higher amounts. Theoretical BCG and CR maximum sorption capacities estimated by the Langmuir model were of 12.02±0.72 mg/g and 9.49±0.79 mg/g for the C1R composite, and of 25.48±2.01 mg/g and 16.78±1.34 mg/g for C2R composite, respectively, values which are in very good agreement with the experimental data. The Freundlich isotherm model described well the sorption process, indicating that the surface of the core-shell sorbents is heterogeneous. Moreover, the sorption of BCG and CR was described well by both pseudo-first order and pseudo-second order kinetic models. Optimum pH for dye desorption was found to be pH 12, CR being desorbed in a higher percentage than BCG.

REFERENCES

[1] P. H. Gleick, *Science*, **302**, 1524 (2003).
[2] G. M. Geise, H.-S. Lee, D. J. Miller, B. D. Freeman, J. E. McGrath *et al.*, *J. Polym. Sci. B*, **48**, 1685 (2010).
[3] A. Lee, J. W. Elam and S. B. Darling, *Environ. Sci.: Water Res. Technol.*, **2**, 17 (2016).
[4] Y. Ying, W. Ying, Q. Li, D. Meng, G. Ren *et al.*, *Appl. Mater. Today*, **7**, 144 (2017).
[5] B. Berrima, W. Maatar, G. Mortha, S. Boufi, L. El Aloui *et al.*, *Cellulose Chem. Technol.*, **50**, 701 (2016).
[6] N. Pandey, S. K. Shukla and N. B. Singh, *Nanocomposites*, **3**, 47 (2017).
[7] A. L. McGaughey, R. D. Gustafson and A. E. Childress, *J. Membr. Sci.*, **543**, 143 (2017).
[8] P. S. Goh, W. J. Lau, M. H. D. Othman and A. F. Ismail, *Desalination*, **425**, 130 (2018).
[9] E. S. Dragan, *Chem. Eng. J.*, **243**, 572 (2014).
[10] S. De Gisi, G. Lofrano, M. Grassi and M. Notarnicola, *Sustain. Mater. Technol.*, **9**, 10 (2016).
[11] E. S. Dragan, D. Humelnicu, M. V. Dinu and R. I. Olariu, *Chem. Eng. J.*, **330**, 675 (2017).
[12] M. Niculaua, B. I. Cioroiu, A. M. Tomoiagă, M. E. Cioroiu and M. I. Lazar, *Cellulose Chem. Technol.*, **51**, 1 (2017).
[13] M. Wawrzkiewicz, *Chem. Eng. J.*, **217**, 414 (2013).
[14] F. Bucatariu, C.-A. Ghiorghita and E. S. Dragan, *Colloid. Surf. A*, **537**, 53 (2018).

[15] G. Decher, *Science*, **277**, 1232 (1997).
[16] F.-X. Xiao, M. Pagliaro, Y.-J. Xu and B. Liu, *Chem. Soc. Rev.*, **45**, 3088 (2016).
[17] S. Zhang, W. Liu, J. Liang, X. Li, W. Liang *et al.*, *Cellulose*, **20**, 1135 (2013).
[18] C. Tian, C. Zhang, H. Wu, Y. Song, J. Shi *et al.*, *J. Mater. Chem. B*, **2**, 4346 (2014).
[19] I. C. Gifu, M. E. Maxim, A. Iovescu, L. Aricov, E. L. Simion *et al.*, *Appl. Surf. Sci.*, **412**, 489 (2017).
[20] A. D. Cramer, W.-F. Dong, N. L. Benbow, J. L. Webber, M. Krasowska *et al.*, *Phys. Chem. Chem. Phys.*, **19**, 23781 (2017).
[21] J. Baettig, J. Oh, J. Bang and A. Khan, *Macromol. Res.*, **25**, 1091 (2017).
[22] C.-A. Ghiorghita, F. Bucatariu and E. S. Dragan, *Cellulose Chem. Technol.*, **48**, 247 (2014).
[23] W. Feng, W. Nie, C. He, X. Zhou, L. Chen *et al.*, *ACS Appl. Mater. Interfaces*, **6**, 8447 (2014).
[24] J. M. Silva, J. R. García, R. L. Reis, A. J. García and J. F. Mano, *Acta Biomater.*, **51**, 279 (2017).
[25] W. Sun, G. Chen, F. Wang, Y. Qin, Z. Wang *et al.*, *Carbohyd. Polym.*, **181**, 183 (2018).
[26] Y. Ma, Y. Zhang, B. Wu, W. Sun, Z. Li *et al.*, *Angew. Chem. Int. Ed.*, **50**, 6254 (2011).
[27] A. Mentbayeva, A. Ospanova, Z. Tashmuhambetova, V. Sokolova and S. Sukhishvili, *Langmuir*, **28**, 11948 (2012).
[28] J. de Grooth, R. Oborný, J. Potreck, K. Nijmeijer and W. M. de Vos, *J. Membr. Sci.*, **475**, 311 (2015).
[29] L. Wang, N. Wang, J. Li, J. Li, W. Bian *et al.*, *Sep. Purif. Technol.*, **160**, 123 (2016).
[30] E. S. Dragan, F. Bucatariu and G. Hitruc, *Biomacromolecules*, **11**, 787 (2010).
[31] F. Bucatariu, C.-A. Ghiorghita, F. Simon, C. Bellmann and E. S. Dragan, *Appl. Surf. Sci.*, **280**, 812 (2013).
[32] F. Bucatariu, C.-A. Ghiorghita, A.-I. Cocarta and E. S. Dragan, *Appl. Surf. Sci.*, **390**, 320 (2016).
[33] E. S. Dragan and I. A. Dinu, *Eur. Polym. J.*, **47**, 1065 (2011).
[34] C.-A. Ghiorghita, F. Bucatariu and E. S. Dragan, *Int. J. Biol. Macromol.*, **107**, 1584 (2018).
[35] Y. Li, J.-Q. Shi, R.-J. Qu, M.-B. Feng, F. Liu *et al.*, *Ecotoxicol. Environ. Saf.*, **86**, 132 (2012).
[36] E. S. Dragan and D. F. Apopei Loghin, *Chem. Eng. J.*, **234**, 211 (2013).
[37] M. Adusumilli and M. L. Bruening, *Langmuir*, **25**, 7478 (2009).
[38] L. Richert, P. Lavalle, E. Payan, X. Z. Shu, G. D. Prestwich *et al.*, *Langmuir*, **20**, 448 (2004).
[39] G. Limousin, J. P. Gaudet, L. Charlet, S. Szenknect, V. Barthès *et al.*, *Appl. Geochem.*, **22**, 249 (2007).